Akif Eren Tatli[1]
Department of Mechanical and Industrial Engineering,
Northeastern University,
Boston, MA 02115
e-mail: tatli.a@northeastern.edu

Dongchuan You
Department of Mechanical and Industrial Engineering,
Northeastern University,
Boston, MA 02115
e-mail: you.d@northeastern.edu

Ashkan Ghanavati
Department of Mechanical and Industrial Engineering,
Northeastern University,
Boston, MA 02115
e-mail: ghanavati.ash@northeastern.edu

Hameed Metghalchi
Department of Mechanical and Industrial Engineering,
Northeastern University,
Boston, MA 02115
e-mail: metghalchi@coe.neu.edu

Insight Into Recompression Brayton Cycle

Recompression cycles have the potential to offer high performance when design parameters such as feasibility, performance, and compactness are considered. These cycles have recently gained attention especially in nuclear and concentrating solar power plants because of their high efficiency and environmentally friendly. A study has been done to investigate and learn more about recompression cycles. In this paper, a recompression Brayton cycle has been analyzed by performing parametric studies on the effectiveness of recuperators, pressure ratio, and split ratio as well as other input variables. To understand the relations between these factors and the performances of the cycle, argon was used as a working fluid because of its constant specific heat. The solution to temperatures at each state has been derived analytically, which is presented as a function of independent input variables. Thermal efficiency and exergy efficiency of this cycle have been determined in these analyses. The model indicates following results: entropy generation of recuperators is lower at a minimum split and decreases with increasing effectiveness. When the cycle is optimized for maximum efficiency it does not operate on maximum specific net work. The energy and exergy efficiencies of the cycle increase with increasing pressure ratio reaching a maximum value at the optimum pressure ratio. The effect of split ratio on temperature difference around recuperators shows that energy recovered at low temperature is higher at a minimum split which yields a higher efficiency in the cycle. The performance of the cycle is strongly affected by turbine inlet temperature. [DOI: 10.1115/1.4062258]

Keywords: energy systems analysis, thermodynamics

1 Introduction

Nowadays, the demand for energy has increased significantly, which raises the attention of fossil energy reserves and environmental problems [1]. Carbon dioxide (CO_2) has been studied as a working fluid in power plants for years because of its favorable high efficiency [2] and environmental safety [3]. There are types of supercritical CO_2 power cycles [4], such as reheating cycle [5], intercooling cycle [5], recompression cycle [6], turbine split flow cycle [7], and few others are described in Refs. [4,8,9]. Mostly, recompression cycle, which was suggested by Feher [10] and Angelino [11], is considered as the most efficient layout of sCO_2. Since compression work around critical point is significantly lower in the sCO_2 cycle and only part of the flow goes through precooler, cycle efficiency increases [12]. Recompression Brayton cycle has been studied both in terrestrial and space applications [13] and proved to have better performances in industries such as bottoming cycles in multipurpose energy production [14], solar energy [15], and nuclear energy [16,17]. The performance of the recompression cycle has been analyzed previously, and its application in different areas has also been discussed recently. You et al. [18] studied the effects of recuperator effectiveness, pressure ratio, and split ratio on cycle performance such as efficiency, exergy efficiency, and energy effectiveness as a bottoming cycle coupled with lithium bromide (aq.) absorption cycle. They stated that combined pressure ratio of top and bottom cycles needs to be determined as well as optimum operating pressures of each layout. Sathish et al. [19] presented results for a 10 MWe with a compressor inlet temperature of 45 °C and discussed its optimal operation strategy. Singh and Mishra [20] presented energy- and exergy-based performance evaluation of a combined cycle of sCO_2 recompression cycle and organic Rankine cycle. Oh et al. [21] discussed an application of sCO_2 recompression cycle in electric thermal energy storage. The calculation for most articles is based on the iteration method in MATLAB, or using other commercial software like ASPEN PLUS, ENGINEERING EQUATION SOLVER (EES), which could only provide numerical solutions but not analytic results. Argon with constant specific heat has been used to understand the behavior of recompression cycles. This model provides the analytical solution of all temperatures in the cycle. Parameters such as minimum and maximum temperatures, compressor efficiency, turbine efficiency, and recuperator effectiveness have been chosen the same as those of sCO_2 recompression cycles. For these reasons, the focus has been on evaluating the effects of pressure ratio and split ratio on the performance of the cycle such as thermal efficiency and exergy efficiency.

In Sec. 2, power cycle model configuration is explained, and in Sec. 3, thermodynamics model has been introduced. In Sec. 4, mathematical model has been developed and equations for temperatures at each state have been derived. In Sec. 5, results have been presented as a function of pressure ratio at each split ratio. Conclusions have been stated in Sec. 6.

2 Model Description

Recompression layout has nine energy conversion devices, including high temperature energy exchanger for energy input, low temperature recuperator (LTR), high temperature recuperators (HTR), a mixing chamber, main compressor, recompression compressor, a turbine, low temperature energy exchanger for transferring energy out of the system (precooler), and a single T-section to split mass flowrates between precooler and recompression. Low-pressure flow is split upon energy rejection at precooler and compressed to a low temperature recuperator at the main compressor. Split flow then mixes with recompressed fraction that is compressed from a parallel compressor into a high temperature side. These two flows then mix in a mixing chamber and enter a high temperature recuperator to recover energy from turbine output (Fig. 1).

3 Thermodynamics Model

Fundamentals of thermodynamics using balance equations have been used to determine the performance of the recompression cycle.

[1]Corresponding author.
Manuscript received January 23, 2023; final manuscript received March 26, 2023; published online April 17, 2023. Assoc. Editor: Reza Sheikhi.

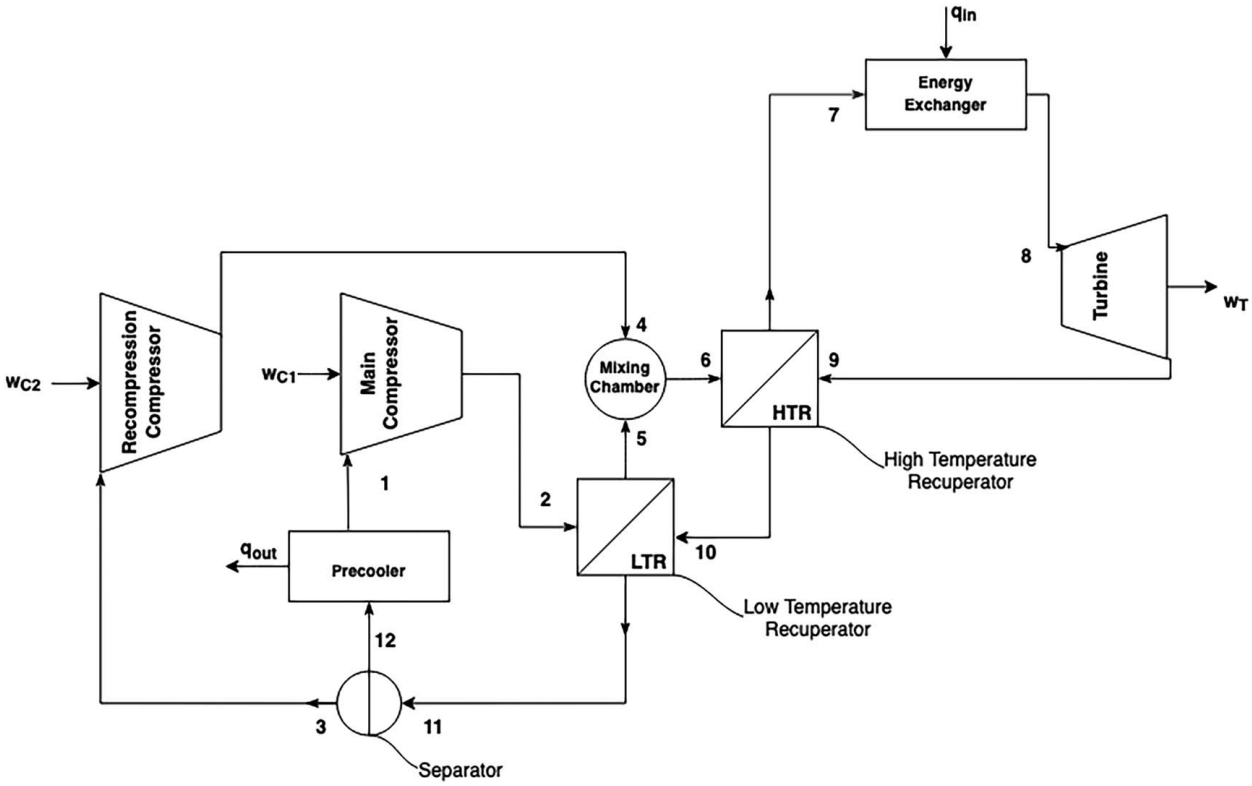

Fig. 1 Recompression Brayton cycle schematic diagram

Energy balance equation:

$$\frac{dU}{dt} = \dot{Q} - \dot{W} + \sum_i \dot{m}_i h_i - \sum_e \dot{m}_e h_e \tag{1}$$

Entropy balance equation:

$$\frac{dS}{dt} = \int \left(\frac{\dot{\delta Q}}{T}\right)_b + \sum_i \dot{m}_i s_i - \sum_e \dot{m}_e s_e + \dot{\sigma} \tag{2}$$

Energy balance has been simplified for different subsystems in the cycle.

Low temperature recuperator energy balance:

$$x(h_2 - h_5) + (h_{10} - h_{11}) = 0 \tag{3}$$

where x is the split ratio defined as the percentage of the total mass flowrate that goes through the main compressor, $x = \dot{m}_{12}/\dot{m}_{11}$.

High temperature recuperator energy balance:

$$(h_6 - h_7) + (h_9 - h_{10}) = 0 \tag{4}$$

Mixing chamber energy balance:

$$(1 - x)h_4 + xh_5 - h_6 = 0 \tag{5}$$

Definition of turbine and compressor efficiencies:

$$\eta_t = \frac{h_8 - h_9}{h_8 - h_{9s}} \tag{6}$$

$$\eta_{c1} = \frac{h_{2s} - h_1}{h_2 - h_1} \tag{7}$$

$$\eta_{c2} = \frac{h_{4s} - h_3}{h_4 - h_3} \tag{8}$$

Definition of effectiveness of recuperators:

$$\varepsilon_{\mathrm{LTR}} = \frac{x(h_5 - h_2)}{h_{10} - h_2} \tag{9}$$

$$\varepsilon_{\mathrm{HTR}} = \frac{h_7 - h_6}{h_9 - h_6} \tag{10}$$

Energy and exergy inputs of the cycle:

$$q_{in} = h_8 - h_7 \tag{11}$$

$$e_x = q_{in}\left(1 - \frac{T_0}{T_s}\right) \tag{12}$$

where T_0 is temperature of surrounding, and T_s is temperature of energy source.

Net work of the cycle per unit mass flowrate:

$$w_{net} = (h_8 - h_9) - x(h_2 - h_1) - (1 - x)(h_4 - h_3) \tag{13}$$

Energy loss:

$$q_{out} = x(h_{12} - h_1) \tag{14}$$

Thermal and exergy efficiencies:

$$\eta = \frac{w_{net}}{q_{in}} = 1 - \frac{q_{out}}{q_{in}} \tag{15}$$

$$\eta_x = \frac{w_{net}}{e_x} \tag{16}$$

Specific enthalpy and entropy of a perfect gas:

$$h(T) - h_o = c_p(T - T_o) \tag{17}$$

where h_o: reference enthalpy at 0 K which is 0 kJ/kg and T_o: reference temperature (0 K)

$$s(T, p) - s_o = c_p \ln \frac{T}{T_o} - R \ln \frac{p}{p_o} \tag{18}$$

Relationship between temperature and pressure for an isentropic process of a perfect gas:

$$Tp^{(k-1)/k} = \text{constant} \tag{19}$$

where k is the specific heat ratio of a perfect gas. Value for specific heats of argon at constant pressure and volume, $c_p = 0.5203$ kJ/kg · K, $c_v = 0.3122$ kJ/kg · K, and $k = 5/3$.

Exit temperature of turbine and compressors:

$$T_9 = T_8(1 - \eta_t(1 - r_p^{-\lambda})) \tag{20}$$

$$T_2 = T_1(1 + (r_p^{\lambda} - 1)/\eta_c) \tag{21}$$

where r_p is pressure ratio and is equal to $p_2/p_1 = p_4/p_3 = p_8/p_9$ and $\lambda = (k-1)/k$.

4 Solution to the Thermodynamic Model

A stand-alone recompression layout has nine energy conversion devices and twelve states in which flow at low pressure side splits before entering two parallel compressors. Split ratio is defined as fraction of total mass flowrate, x, which enters precooler. The model includes eight equations and eight unknowns for temperatures. Temperatures after turbine, T_9, and main compressor temperature, T_2 are independent of flowrate and are determined using Eqs. (20) and (21). The remaining six temperatures are determined using Eqs. (22)–(27). Pressure drops, kinetic and potential energy change across pipes and energy exchangers have been neglected. Both main compressor and recompression compressor operate under the same pressure ratio.

$$\eta_c(T_4 - T_3) - T_3(r_p^{\lambda} - 1) = 0 \tag{22}$$

$$x(T_2 - T_5) + (T_{10} - T_3) = 0 \tag{23}$$

$$(T_6 - T_7) + (T_9 - T_{10}) = 0 \tag{24}$$

$$x(T_5 - T_2) - \varepsilon_L(T_{10} - T_2) = 0 \tag{25}$$

$$(T_7 - T_6) - \varepsilon_H(T_9 - T_6) = 0 \tag{26}$$

$$(1 - x)T_4 + xT_5 - T_6 = 0 \tag{27}$$

Equations (22)–(27) have been solved analytically, and the results for six temperatures T_3, T_4, T_5, T_6, T_7, T_{10} are shown.

$$T_3 = T_{10} + \varepsilon_L(T_2 - T_{10}) \tag{28}$$

$$\begin{aligned} T_4 = {} & T_1\varepsilon_L(X + Yr_p^{\lambda}) + (1 - \varepsilon_L)(T_8(\varepsilon_H - 1)((X + Yr_p^{\lambda})A \\ & + (Xr_p^{-\lambda} + Y)B) + T_1\varepsilon_L\varepsilon_H(C + Dr_p^{\lambda} \\ & + Er_p^{2\lambda})(X + Yr_p^{\lambda}))/(F + Gr_p^{\lambda}) \end{aligned} \tag{29}$$

$$T_5 = T_2(1 - \varepsilon_L/x) + T_{10}\varepsilon_L/x \tag{30}$$

$$\begin{aligned} T_6 = {} & T_1(x - \varepsilon_L)(C' + D'r_p^{\lambda} + Er_p^{2\lambda}) - T_1x(C'' + D''r_p^{\lambda} + Er_p^{2\lambda}) \\ & - (T_8(a + br_p^{\lambda})(\varepsilon_H - 1)(A + Br_p^{-\lambda}) + T_1\varepsilon_L\varepsilon_H(a + br_p^{\lambda}) \\ & (C + Dr_p^{\lambda} + Er_p^{2\lambda}))/(F + Gr_p^{\lambda}) \end{aligned} \tag{31}$$

$$\begin{aligned} T_7 = {} & T_8\varepsilon_H(A + Br_p^{-\lambda}) + (\varepsilon_H - 1)(T_1\varepsilon_L(C + Dr_p^{\lambda} + Er_p^{2\lambda}) \\ & + (T_8(a + br_p^{k})(\varepsilon_H - 1)(A + Br_p^{-\lambda}) \\ & + T_1\varepsilon_L\varepsilon_H(a + br_p^{\lambda})(C + Dr_p^{\lambda} + Er_p^{2\lambda}))/(F + Gr_p^{\lambda}) \end{aligned} \tag{32}$$

$$T_{10} = (T_8(\varepsilon_H - 1)(A + Br_p^{-\lambda}) + T_1\varepsilon_L\varepsilon_H(C + Dr_p^{\lambda} + Er_p^{2\lambda}))/(F + Gr_p^{\lambda}) \tag{33}$$

where X, Y, A, B, C, D, E, F, G, C', C'', D', D'', a, and b are input parameters

$$X = 1 - 1/\eta_c$$

$$Y = 1/\eta_c$$

$$A = 1 - \eta_t$$

$$B = \eta_t$$

$$C = (1 - 1/\eta_c)(1 + (1 - x)(1 - \eta_c)/\eta_c - x/\varepsilon_L)$$

$$D = (1/\eta_c - 1)(1 - x)/\eta_c + (1 + (1 - x)(1 - \eta_c)/\eta_c - x/\varepsilon_L)$$

$$E = -(1 - x)/\eta_c^2$$

$$F = \varepsilon_H\varepsilon_L - \varepsilon_H((1 - \varepsilon_L)(1 - \eta_c)(1 - x)/\eta_c) - 1$$

$$G = \varepsilon_H(1 - x)(1 - \varepsilon_L)/\eta_c$$

$$C' = (1 - 1/\eta_c)(1 + (1 - \eta_c)(1 - x)/\eta_c)$$

$$D' = D + (1 + (1 - \eta_c)(1 - x)/\eta_c)/\eta_c$$

$$C'' = (1 - 1/\eta_c)(1 - \eta_c)(1 - x)/\eta_c$$

$$D'' = (1 - \eta_c)(1 - x)/\eta_c^2$$

$$a = (1 - \varepsilon_L)(1 - x)(1 - \eta_c)/\eta_c - \varepsilon_L$$

$$b = -(1 - \varepsilon_L)(1 - x)$$

Above equations along with Eqs. (15) and (16) have been used to determine thermal efficiency and exergy efficiency. Since the performance of the cycle depends mainly on pressure ratio across the compressors, an equation for optimum pressure ratio was developed. This was achieved by differentiating the equation for efficiency of the cycle with respect to pressure ratio and was set equal to zero.

In order to determine optimum split ratio, an equation has been developed from entropy balance in recuperators.

$$\sigma_{\text{LTR}} = c_p\left[x\ln\left(\frac{T_5}{T_2}\right) + \ln\left(\frac{T_{11}}{T_{10}}\right)\right] \geq 0 \tag{34}$$

$$\sigma_{\text{HTR}} = c_p\left[\ln\left(\frac{T_7}{T_6}\right) + \ln\left(\frac{T_{10}}{T_9}\right)\right] \geq 0 \tag{35}$$

$$\sigma_{\text{Total}} = \sigma_{\text{LTR}} + \sigma_{\text{HTR}} \tag{36}$$

where σ is defined as specific entropy generation.

Figure 2 shows total entropy generation in two recuperators at different split ratios as a function of recuperator effectiveness at a pressure ratio of 1.5. For higher split ratio overall irreversibility is greater in the recuperators. Lower split ratio is bounded with

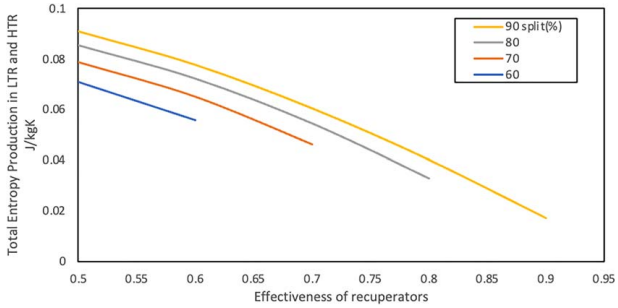

Fig. 2 Total entropy production of recuperators as a function of effectiveness and split ratio

effectiveness of recuperator due to minimum temperature difference at LTR, $T_5 \leq T_{10}$. As it can be seen at a constant effectiveness of recuperators, the lower split ratio results in less entropy production improving performance of the cycle.

5 Results and Discussions

The independent input variables in the system are minimum and maximum temperatures, effectiveness of low and high temperature recuperators, isentropic efficiencies of compressors and turbine, split and pressure ratios across the compressors and turbine. Dependent variables are temperatures at all states and performance of the power cycle such as thermal and exergy efficiencies. Parameters are $T_{\text{source}} = 800\,^{\circ}\text{C}$, $T_{\text{env}} = 20\,^{\circ}\text{C}$, $T_{\min} = 25\,^{\circ}\text{C}$, $T_{\max} = 750\,^{\circ}\text{C}$, effectiveness of low and high temperature recuperators, $\varepsilon_{\text{LTR}} = 0.88$, $\varepsilon_{\text{LTR}} = 0.88$, $\eta_c = 0.89$, $\eta_t = 0.9$, and $c_p = 0.57$ kJ/kg · K.

Figure 3 shows net work as a function of pressure ratio for three different splits. Cycle generates highest net work at a higher split ratio at which both energy input and energy rejection increase but increase of energy input is higher than energy rejection. Work required for compression is also lower due to lower fraction of split in recompressor. Moreover, net work increases with increasing pressure ratio up to a limit at which the maximum limit has been determined from entropy balance in HTR. This limit has been found for minimum split which yields the highest thermal-to-electric efficiency in the cycle.

Figure 4 shows cycle efficiency as a function of pressure ratio at three different split ratios. The highest efficiency has shown at a minimum split. Even a slight difference from the optimum drops the efficiency and at some pressure ratio split curves crosses and decreases in minimum split becomes greater. It can also be seen that optimum pressure ratio at minimum split ratio is smaller.

Figure 5 shows cycle exergy efficiency as a function of pressure ratio at three different split ratios. It has been observed that exergy efficiency decreases with increasing pressure ratio beyond the optimum pressure ratio.

Figure 6 indicates that increasing pressure ratio leads to a higher increment in energy input than that of net work. This explains the downward trend in cycle performance beyond the optimum pressure.

Figure 7 shows that ratio of total load, defined as amount of energy transferred from high temperature argon to low temperature argon, in recuperators to energy input to the cycle decreases with increasing pressure ratio and is almost independent of split ratio.

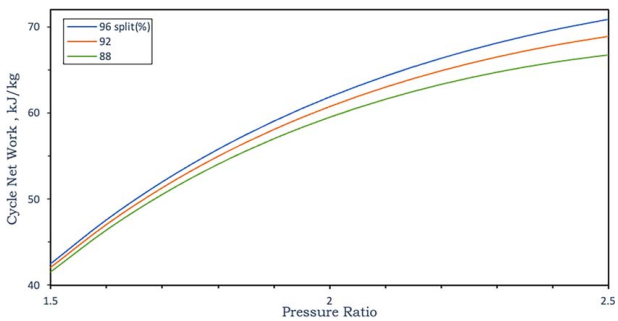

Fig. 3 Cycle specific net work output as a function of pressure ratio

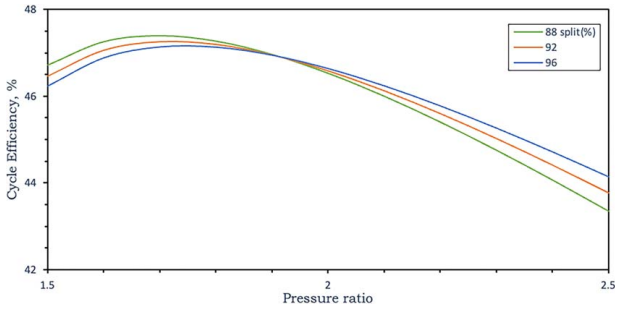

Fig. 4 Cycle efficiency as a function of pressure ratio

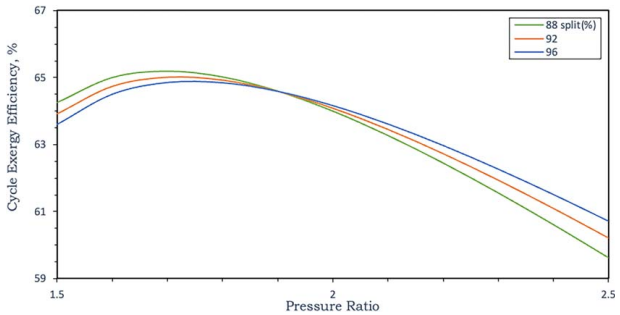

Fig. 5 Cycle exergy efficiency as a function of pressure ratio

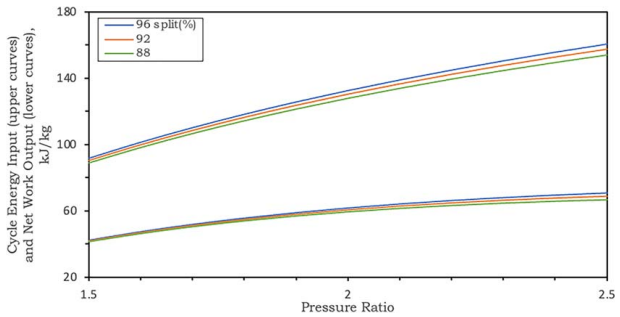

Fig. 6 Cycle energy input (upper curves) and cycle net work (lower curves) as a function of pressure ratio

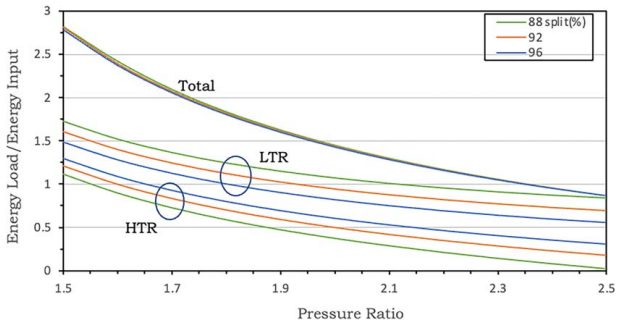

Fig. 7 Ratio of energy load in recuperators to energy input as a function of pressure ratio at each split. Split ratios represent load ratio of Total, LTR, and HTR.

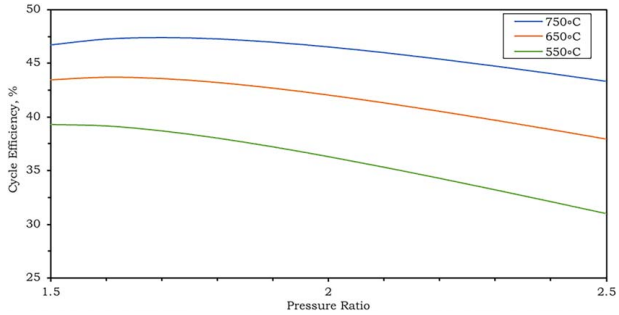

Fig. 8 Cycle efficiency at different turbine inlet temperatures as a function of pressure ratio

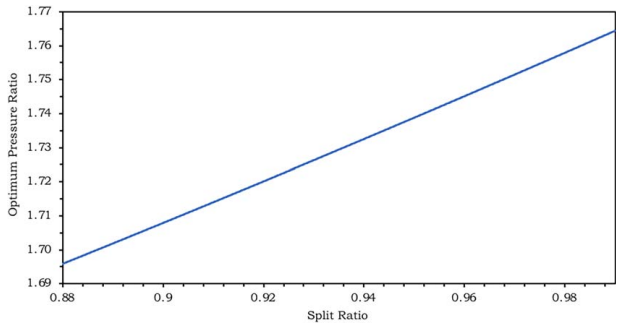

Fig. 9 Cycle optimum pressure ratio as a function of split ratio

The ratio of energy load in LTR is higher than HTR at all pressure ratios. At a constant pressure ratio, the load ratio is greater in LTR and smaller in HTR at a minimum split ratio. This implies that temperature difference around LTR is significantly higher than HTR so is irreversibility.

Figure 8 shows energy efficiency of the cycle as a function of pressure ratio at different turbine inlet temperatures. It can be seen when turbine inlet temperature increases, the efficiency increases significantly, which is consistent with other Brayton cycles. It also shows that there is an optimum pressure ratio which increases as turbine inlet temperature increases. This is consistent with the work of Hiller [22].

Figure 9 shows the relation between cycle optimum pressure ratio for maximum efficiency as a function of split ratio. For an ideal cycle, the relation is almost linear. As it can be seen, by increasing the split ratio the optimum pressure ratio (the pressure ratio for maximum cycle efficiency) also increases. This implies the cycle requires higher operating pressures by increasing the amount of flow sent to low temperature recuperator.

6 Conclusion

Recompression cycle depends mainly on factors such as effectiveness of recuperators, split ratio, turbine inlet temperature, and pressure ratio. In this work, we studied the effect of pressure ratio and split ratio on an ideal recompression Brayton cycle. Thermodynamics model was developed from energy and entropy balance equations resulting in a linear set of equations for temperatures at different states of the cycle. Temperatures at different states within the cycle have been calculated.

The following conclusions can be made:

(1) Increasing effectiveness of recuperators decreases total entropy generation in the cycle.
(2) Cycle net work increases as a function of pressure ratio.
(3) Energy efficiency as well as exergy efficiency becomes maximum at optimum pressure ratio.
(4) At the optimum pressure ratio, however, net work is not maximum.
(5) Lower split ratio increases cycle energy efficiency at optimum pressure ratio.
(6) Total energy recovery for all splits is almost equal but energy recovery at HTR is smaller at a minimum split and greater in LTR.
(7) Cycle efficiency increases as turbine inlet temperature increases.
(8) Optimum pressure ratio increases with increasing turbine inlet temperature.

Conflict of Interest

There are no conflicts of interest. This article does not include research in which human participants were involved. Informed consent not applicable. This article does not include any research in which animal participants were involved.

Data Availability Statement

The datasets generated and supporting the findings of this article are obtainable from the corresponding author upon reasonable request.

Nomenclature

e = exergy
k = specific heat ratio
q = heat
s = entropy
T = temperature
$\dot{m}$ = mass flowrate
r_p = pressure ratio
η = efficiency of the cycle

Subscripts

e = outlet
h = enthalpy
i = inlet
p = pressure
t = turbine
w = work
x = split ratio
c_p = ideal gas constant specific heat
$c1$ = main compressor
$c2$ = recompression compressor
ε = recuperator effectiveness
$\dot{\sigma}$ = entropy production rate
HTR = high temperature recuperator
LTR = low temperature recuperator

References

[1] Tietenberg, T., and Lewis, L., 2018, *Environmental and Natural Resource Economics*, Routledge, Abingdon, Oxfordshire, UK.
[2] Ahn, Y., Bae, S. J., Kim, M., Cho, S. K., Baik, S., Lee, J. I., and Cha, J. E., 2015, "Review of Supercritical CO_2 Power Cycle Technology and Current Status of Research and Development," Nucl. Eng. Technol., **47**(6), pp. 647–661.
[3] Sarkar, J., 2015, "Review and Future Trends of Supercritical CO_2 Rankine Cycle for Low-Grade Heat Conversion," Renew. Sustain. Energy Rev., **48**, pp. 434–451.
[4] Crespi, F., Gavagnin, G., Sánchez, D., and Martínez, G. S., 2017, "Supercritical Carbon Dioxide Cycles for Power Generation: A Review," Appl. Energy, **195**, pp. 152–183.
[5] Turchi, C. S., Ma, Z., Neises, T., and Wagner, M., 2012, "Thermodynamic Study of Advanced Supercritical Carbon Dioxide Power Cycles for High Performance Concentrating Solar Power Systems," ASME 2012 6th International Conference on Energy Sustainability, San Diego, CA, July 23–26, American Society of Mechanical Engineers.
[6] Turchi, C. S., Ma, Z., Neises, T. W., and Wagner, M. J., 2013, "Thermodynamic Study of Advanced Supercritical Carbon Dioxide Power Cycles for Concentrating Solar Power Systems," ASME J. Sol. Energy Eng., **135**(4), p. 041007.

[7] Vesely, L., Manikantachari, K. R. V., Vasu, S., Kapat, J., Dostal, V., and Martin, S., 2019, "Effect of Impurities on Compressor and Cooler in Supercritical CO_2 Cycles," ASME J. Energy Resour. Technol., **141**(1), p. 012003.
[8] Bai, Z., Zhang, G., Yang, Y., and Wang, Z., 2019, "Design Performance Simulation of a Supercritical CO_2 Cycle Coupling With a Steam Cycle for Gas Turbine Waste Heat Recovery," ASME J. Energy Resour. Technol., **141**(10), p. 102001.
[9] Khadse, A., Blanchette, L., Kapat, J., Vasu, S., Hossain, J., and Donazzolo A., 2018, "Optimization of Supercritical CO_2 Brayton Cycle for Simple Cycle Gas Turbines Exhaust Heat Recovery Using Genetic Algorithm," ASME J. Energy Resour. Technol., **140**(7), p. 071601.
[10] Feher, E. G., 1967, *The Supercritical Thermodynamic Power Cycle*, IECEC, Miami Beach, FL.
[11] Angelino, G., 1968, "Carbon Dioxide Condensation Cycles for Power Production," J. Eng. Power, **90**(3), pp. 287–295.
[12] You, D., and Metghalchi, H., 2021, "On the Supercritical Carbon Dioxide Recompression Cycle," ASME J. Energy Resour. Technol., **143**(12), p. 121701.
[13] Miao, X., Zhang, H., Zhang, D., Zhang, C., and Huang, Z., 2022, "Properties of Nitrous Oxide and Helium Mixtures for Space Nuclear Recompression Brayton Cycle," Energy Rep., **8**, pp. 2480–2489.
[14] You, D., and Metghalchi, H., 2022, "Analysis of Aqueous Lithium Bromide Absorption Refrigeration Systems," ASME J. Energy Resour. Technol., **144**(1), p. 012105.
[15] Yu, T., and Song, Y., 2022, "Analysis and Performance Optimization of Supercritical CO_2 Recompression Brayton Cycle Coupled Organic Rankine Cycle Based on Solar Tower," ASME J. Sol. Energy Eng., **144**(5), p. 051007.
[16] Dostal, V., Driscoll, M. J., and Hejzlar, P., 2004, *A Supercritical Carbon Dioxide Cycle for Next Generation Nuclear Reactors*, Massachusetts Institute of Technology, Cambridge, MA.
[17] Syblik, J., Vesely, L., Entler, S., Dostal, V., and Stepanek, J., 2019, "Advanced S-CO_2 Brayton Power Cycles in Nuclear and Fusion Energy," ASME Turbo Expo 2019: Turbomachinery Technical Conference and Exposition, Phoenix, AZ, June 17–21.
[18] You, D., Tatli, A. E., Ghanavati, A., and Metghalchi, H., 2022, "Design and Analysis of a Solar Energy Driven Tri-Generation Plant for Power, Heating, and Refrigeration," ASME J. Energy Resour. Technol., **144**(8), p. 082105.
[19] Sathish, S., Kumar, P., and Nassar, A., 2021, "Analysis of a 10 MW Recompression Supercritical Carbon Dioxide Cycle for Tropical Climatic Conditions," Appl. Therm. Eng., **186**, p. 116499.
[20] Singh, H., and Mishra, R., 2018, "Energy-and Exergy-Based Performance Evaluation of Solar Powered Combined Cycle (Recompression Supercritical Carbon Dioxide Cycle/Organic Rankine Cycle)," Clean Energy, **2**(2), pp. 140–153.
[21] Oh, S., Oh, B. S., and Lee, J. I., 2022, "Performance Evaluation of Supercritical Carbon Dioxide Recompression Cycle for High Temperature Electric Thermal Energy Storage," Energy Convers. Manage., **255**, p. 115325.
[22] Hiller, C. C., 1978, "A Sensitivity of Brayton Cycle Power Plant Performance," Sandia Laboratories Energy Report.